Chemical Science

ROYAL SOCIETY OF CHEMISTRY

EDGE ARTICLE

View Article Online
View Journal

Cite this: DOI: 10.1039/d5sc08677a

All publication charges for this article have been paid for by the Royal Society of Chemistry

Pushing the boundaries of BODIPY chemistry: 2-(dimethylamino)methyl BODIPYs as enablers of diversification with nucleophiles

Sergio Serrano-Buitrago, [a] Carla Marcos,[a] Natalia Casado, [b] Andrea Aranda,[a] Florencio Moreno, [a] Jorge Bañuelos, [b] David Valdivieso González, [c] Iván López-Montero, [cde] Beatriz L. Maroto *[a] and Santiago de la Moya *[a]

The BODIPY family of organic dyes has emerged as a versatile platform in photonic materials science, driven by their outstanding photophysical properties and the synthetic flexibility of BODIPY chemistry. Post-functionalization strategies have been pivotal in expanding BODIPY's application scope. However, current methodologies for rapid diversification with nucleophiles suffer from key limitations, including the use of unstable intermediates, limited substrate scope, and reliance on hazardous or costly reagents. In this work, we introduce 2-(dimethylamino)methyl BODIPYs as novel, stable, and easily accessible electrophilic intermediates that enable efficient BODIPY diversification with a broad range of neutral protic nucleophiles *via* unimolecular nucleophilic substitution. These intermediates are straightforwardly synthesized from highly common and accesible 2-unsubstituted BODIPYs through electrophilic aromatic substitution using inexpensive Eschenmoser's salt, and can be activated under mild conditions *via* simple amine quaternization. Importantly, this strategy is compatible with 3,5-dimethylated BODIPYs, preserving access to Knoevenagel-like BODIPY chemistry for large chromophore π-extension towarsds bathochromic shift into the red-to-NIR spectral region. The efficacy of this methodology is demonstrated through the synthesis of a number of BODIPY dyes with diverse substitution patterns and selectable photophysical behavior. Furthermore, we highlight its practical utility through the design of functional BODIPY derivatives, including ICT-based fluorescent pH indicators, fluorogenic acidotropic bioprobes, and water-soluble laser dyes.

Received 7th November 2025
Accepted 7th February 2026

DOI: 10.1039/d5sc08677a

rsc.li/chemical-science

Introduction

The BODIPY (boron-dipyrromethene) family of organic dyes has become a cornerstone in photonic research, driving innovation across a wide range of applications of high socio-economic relevance.[1] This prominence stems from their exceptional photophysical behaviours, particularly their strong fluorescence, combined with their synthetic accessibility and versatile tunability *via* a set of well-established, straightforward organic-chemistry transformations collectively referred to as BODIPY chemistry.[2]

Within the BODIPY-chemistry framework, post-functionalization strategies have proven particularly powerful for expanding the structural diversity and functional utility of BODIPY dyes.[2f,k,m,o,r] These strategies not only allow precise tuning of key photophysical properties, such as absorption and emission wavelengths or fluorescence efficiencies, but also enable the introduction of essential functional features, including water solubility,[3] biorecognition capability for bioimaging and medical applications,[4] or selective reactivity for chemical sensing.[5] They also promote non-standard BODIPY photophysics, such as triplet-state population[6] (relevant for photodynamic therapy,[7] photon up-conversion,[8] or photocatalysis[9]), efficient chiroptical responses of the inherently achiral BODIPY chromophore, including circularly polarized luminescence,[10] or enhanced optoelectronic behaviours including OLED illumination,[11] thereby significantly broadening the scope of BODIPY-based materials for a wide range of advanced photonic applications.

Since most common BODIPY post-functionalization strategies affect the chromophoric core, they can substantially alter the dye's photophysical properties.[2f,k,m] This presents a limitation when the goal is to introduce key functional moieties—

[a]Departamento de Química Orgánica, Facultad de Ciencias Químicas, Universidad Complutense de Madrid, Ciudad Universitaria S/N, Madrid 28040, Spain. E-mail: santmoya@ucm.es

[b]Departamento de Química-Física, Universidad del País Vasco-EHU, Bilbao 48080, Spain

[c]Departamento de Química Física, Facultad de Ciencias Químicas, Universidad Complutense de Madrid, Ciudad Universitaria S/N, 28040 Madrid, Spain

[d]Instituto de Investigación Biomédica Hospital Doce de Octubre (imas12), Avda. de Córdoba S/N, 28041, Madrid, Spain

[e]Instituto Pluridisciplinar, Universidad Complutense de Madrid, Pº Juan XXIII 1, 28040, Madrid, Spain

such as for biorecognition—into a photophysically optimal BODIPY dye.[4] In this context, the introduction of highly reactive functional groups, such as halogens, pseudohalogens, activated carboxyls, formyls, alkynes, or azides, at peripheral BODIPY positions (*i.e.*, positions electronically isolated from the chromophore by an appropriate covalent spacer) is particularly attractive, as it generally preserves the dye's intrinsic photophysics.[2f,k,m,4] However, spacer-based post-functionalization strategies, often involving BODIPY *meso*-phenyl or 3-styryl positions, typically require multi-step synthetic sequences, which can significantly reduce overall efficiency.[2f,k,m,4]

In this context, special attention should be given to the bimolecular nucleophilic substitution (S_N2) reactions of 3-(bromomethyl) and 3,5-bis(bromomethyl) BODIPYs with neutral protic nucleophiles (NuH), particularly organic nucleophiles, as introduced by Ulrich and Ziessel in 2012 (Scheme 1).[12] This methylene-spacer strategy offers rapid access to a wide range of asymmetric and symmetric BODIPY derivatives, since the key, reactive bromomethyl BODIPY intermediates are straightforwardly generated by electrophilic bromination of 3/5-methylated BODIPYs (enol-type BODIPY chemistry).[12] However, the method seems to be restricted to sufficiently reactive heteroatom-based nucleophiles. Additionally, it seems to require electron-deficient (*meso*-iodoarylated) persubsituted BODIPYs,[12] likely to activate the S_N2 reaction and prevent BODIPY bromination by aromatic electrophilic substitution (S_EAr). Moreover, the key bromomethylated intermediates (*i.e.*, the electrophilic enablers of diversification with nucleophiles) are unstable and non-isolable, requiring bromination and substitution to be conducted sequentially in a one-pot protocol for each transformation (Scheme 1).[12]

To address these limitations, Martínez–Martínez, Chiara, Chiara and co-workers later proposed a more robust methylene-spacer strategy, which is based on 3-(acetoxymethyl) BODIPY as alternative, stable and isolable, electrophilic enabler.[13] Notably, under Lewis acid activation, these compounds are proposed to undergo unimolecular nucleophilic substitution (S_N1), enabling reaction with a significantly broader range of organic nucleophiles, including carbon-based ones (Scheme 1).[13] However, this strategy requires starting from non-conventional 4,4-dicyano BODIPYs (*CN*-BODIPYs) instead of common 4,4-difluoro BODIPYs (*F*-BODIPYs), likely to prevent dye decomposition during the substitution step (and probably, competitive at-boron substitution of fluorines). Besides, it uses potentially hazardous reagents such as tin tetrachloride and trimethylsilyl cyanide to generate the key *CN*-BODIPY from the corresponding *F*-BODIPY, lead tetraacetate for achieving the required oxidative BODIPY-methyl acetoxylation, and the expensive, rare-earth-based scandium triflate catalyst to generate the key (BODIPY-3-yl)methyl cation (see Scheme 1).[13] Moreover, it seems to require persubstituted BODIPYs, likely to prevent competitive S_EAr reactions at the BODIPY core.[13] Furthermore, it cannot be applied to certain nucleophiles, particularly amine-based nucleophiles likely due to their strong coordination with the required Lewis acid.[13] It must be also noted here that the involved (BODIPY-3-yl)methyl cation must be significantly unstable owing to acidic nature of the BODIPY 3-methyl position. Together, these factors may substantially limit the practical applicability of this otherwise powerful functionalization method.

Additionally, using the BODIPY 3/5-methyls for enabling BODIPY post-functionalization with nucleophiles blocks valuable BODIPY-chromophore π-extension *via* Knoevenagel-type double condensation of 3,5-dimethyl BODIPYs with aromatic aldehydes, which is the most widely used strategy to easily achieve strong bathochromic shifts of the BODIPY absorption/emission bands.[2d,4a,14] This is a big drawback in applications that require BODIPYs acting in the red-to-NIR region of the electromagnetic spectrum, such as certain bio-medical or optical communication applications.[2d,4a,14]

To address all these limitations, while keeping the advantage of the S_N1 processes to enable BODIPY diversification with a broad range of neutral protic nucleophiles, we hypothesized on the alternative use of (BODIPY-2-yl)methyl cations. On the one hand, these carbocations should be more stable than the (BODIPY-3-yl)methyl counterparts and, therefore, they should be easier to generate. On the other hand, potential 3/5-methyl groups would remain available for enol-type BODIPY chemistry, particularly Knoevenagel-type double condensation for spectral red-shifting into the red-NIR region, to be performed either prior to or following the transformation.

To access these BODIPY carbocations, we propose exploiting the nucleophilic character of the BODIPY 2-position, which readily undergoes S_EAr with a plethora or electrophiles,

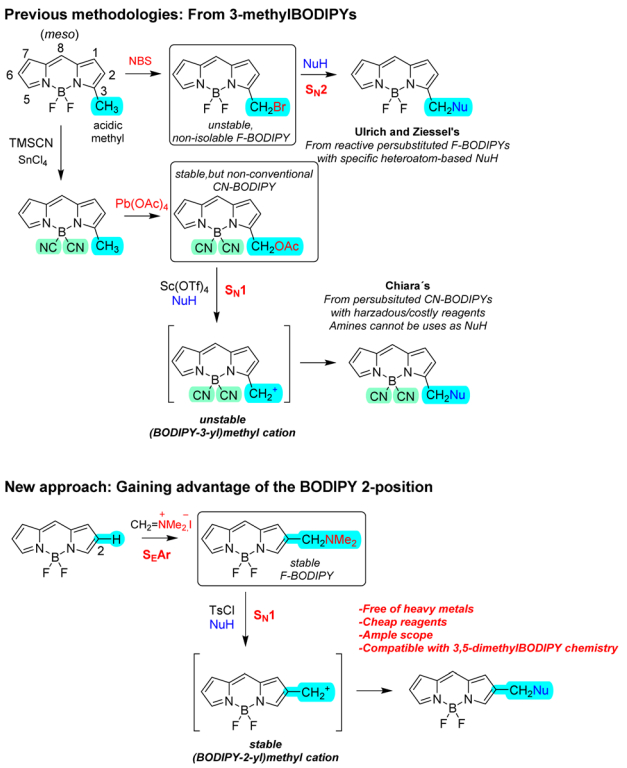

Scheme 1 Comparison of previous methylene-spacer based methodologies for BODIPY post-functionalization with a neutral protic nucleophile (NuH), and the new approach reported herein. Key electrophilic enablers highlighted in boxes.

including C-electrophiles such as one-carbon synthetic equivalents (*e.g.*, Vilsmeier–Haack reagent).[15] In this context, we also hypothesized on the use of the inexpensive and commercially available Eschenmoser's salt (*N*-methyl-*N*-methylenemethanaminium iodide) as one-carbon electrophilic synthetic equivalent to directly generate 2-(dimethylamino) methyl BODIPYs from 2-unsusbtituted BODIPYs by S_EAr. These intermediates could then be activated for the desired S_N1 reaction with NuH *via* simple quaternization of the dimethylamino group.[16] Nonetheless, the π-accelerated S_N2 should not be discarded at the working reaction mechanism.

In this work, we demonstrate this possibility by reporting the effectiveness of 2-(dimethylamino)methyl BODIPYs as enablers of BODIPY diversification with an ample variety of NuHs under mild reaction conditions and without using hazardous and/or costly reagents or catalysts, showcasing some selected applications, particularly the development of valuable ICT-based BODIPY sensors (fluorescent pH indicators and fluorogenic acidotropic bioprobes) and water-soluble BODIPY laser dyes.

Results and discussion

Adjusting the methodology

To test our hypotheses, we selected: known 1,3,5,7-tetramethyl-8-(4-methylphenyl)-*F*-BODIPY (**1**) as the starting reactive BODIPY, standard quaternization with methyl iodide to activate the expected (dimethylamino)methyl-based enabler (**2**), and benzyl alcohol (BnOH) as the neutral nucleophile (Scheme 2).

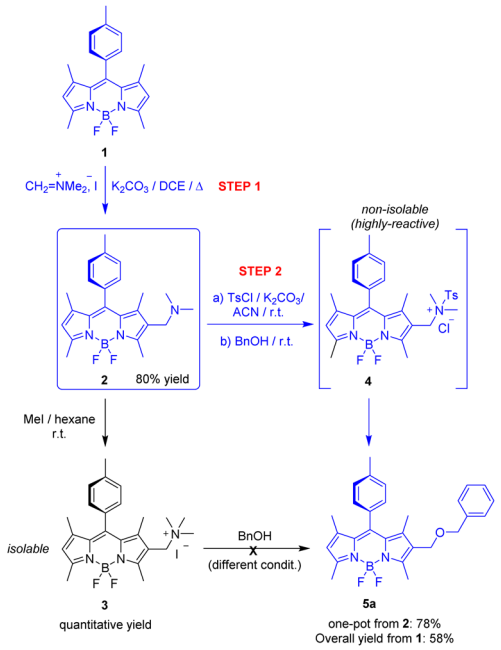

Scheme 2 Chemoselective synthesis of **1**-derived enabler **2**; failed activation as the trimethylammonium salt **3**; and successful activation as the (dimethyl)(tosyl)ammonium salt **4**, which enables reaction with BnOH to generate **5**. In blue, method's route. DCE: 1,2-dichloroethane; ACN: acetonitrile; Ts: tosyl; Bn: benzyl. See the SI for full experimental details.

This selection was made based on the following criteria: (i) the accessibility of the starting materials; (ii) the absence of substitution at BODIPY positions 2 and 6 to probe chemoselectivity during enabler synthesis (mono-S_EAr *vs.* bis-S_EAr); (iii) the presence of substituents (methyls) at BODIPY positions 1 and 3 to evaluate potential steric hindrance effected near the reactive site of the enabler; (iv) the presence of methyls at BODIPY positions 3 and 5, enabling assessment of compatibility with enol-type BODIPY chemistry before or after functionalization.

As shown in Scheme 2, selected BODIPY **1** (synthesized according to the reported procedure[17]) underwent chemoselective aromatic substitution (mono-S_EAr) with Eschenmoser's salt in the presence of potassium carbonate as base in refluxing 1,2-dichloroethane (DCE), affording derivative **2** in 80% yield. Subsequent standard methylation of **2** with methyl iodide in hexane led to the formation of the corresponding trimethylammonium salt in quantitative yield. However, this salt failed to undergo the expected nucleophilic substitution with BnOH under a variety of experimental conditions. Instead, recovery of the starting material, or dye decomposition under harder conditions, was consistently observed.

To address this issue, we explored the activation of **2** as the (dimethyl)(tosyl)ammonium salt **4**. The new ammonium group was expected to serve as a better leaving group than the previous one owing to the strong electron-withdrawing nature of the tosyl ((4-methylphenyl)sulfonyl) moiety. Indeed, this activation—achieved *via* rapid reaction (<5 min) with tosyl chloride (TsCl) at room temperature—proved highly effective. It generated a highly reactive intermediate that could not be isolated from the reaction mixture, but reacted cleanly and rapidly (<3 min, r.t.) with BnOH to furnish BODIPY derivative **5a**. This reactive behaviour strongly supports the *in situ* formation of the (dimethyl)(tosyl)ammonium salt (**4**), and the subsequent generation of the (BODIPY-2-yl)methyl cation by rapid release of *N*,*N*-dimethyltosylamide, which was isolated from the reaction mixture. It must be noted here that the π-accelerated S_N2 mechanism cannot be ruled out based on these results. However, the notably rapid reaction kinetics observed for all the tested neutral nucleophiles, together with previous mechanistic reports on related BODIPY-based substitution reactions,[13] support the proposed S_N1 pathway.

As expected, (dimethylamino)methyl enabler **2** exhibited significantly lower fluorescence than the parent BODIPY **1** (Table 1), with the fluorescence quantum yield (ϕ) decreasing as the polarity of the medium increased (Tables S1 and S2 in the SI).

This behaviour is consistent with photoinduced intramolecular charge transfer (ICT) facilitated by the electron-donating amino group. Support for this mechanism comes from analogous trends observed in related aminomethyl BODIPY systems,[12,13,18] the recovery of the starting fluorescent behaviour in the trimethylammonium derivative **3**, and the intermediate photophysical behaviour of the (benzyloxy)methyl derivative **5a**—consistent with the lower electron-donating ability of the oxygen in **5a** compared to the amine nitrogen in **2**—(see Table 1).

Thanks to its synthetic simplicity and efficiency, relatively low cost, and the absence of hazardous reagents, the two-step

Table 1 Photophysical signatures (maximum absorption, λ_{ab}, and fluorescence, λ_{fl}, wavelength; maximum molar absorption, ε_{max}; fluorescence quantum yield, ϕ; and lifetime, τ) of related BODIPYs **1–3** and **5a** in chloroform, at dye concentration *ca.* 2×10^{-6} M. See the SI for full experimental details

Dye	λ_{ab} (nm)	ε_{max} (M^{-1} cm^{-1})	λ_{fl} (nm)	ϕ	τ (ns)
1	503.0	83 000	513.5	0.60	3.57
2	509.0	86 000	521.0	0.13	0.92[a]
3	500.0	60 000	509.0	0.46	3.15
5a	508.0	84 000	519.0	0.65	3.79

[a] Average lifetime from biexponential fit.

derivatization of 2-unsubstituted BODIPYs into methylene-spaced 2-substituted analogues—through the straightforward synthesis of a 2-[(dimethylamino)methyl]BODIPY enabler (see Scheme 2)—offers a practical and efficient method for diversifying conventional *F*-BODIPYs with organic nucleophiles.

Exploring the scope

Nucleophiles. To explore the nucleophile scope of the proposed chemical methodology, we selected a focused set of NuHs with distinct reactivity profiles. This included various O-nucleophiles (alcohols, phenols and carboxylic acids), N-nucleophiles (primary and secondary alkyl and aryl amines), one representative C-nucleophile (an alkylated pyrrole), and one representative S-nucleophile (thiophenol), all aimed at diversifying compound **1** *via* (dimethylamino)methylated enabler **2**. Fig. 1 shows this BODIPY diversification.

It is important to note that our aim was not to test an exhaustive range of NuH species—since the intermediate (BODIPY-2-yl)methyl cation is expected to react with a wide variety of such nucleophiles, as has been previously reported for the analogous (BODIPY-3-yl)methyl cation.[13] Instead, our goal was to evaluate: (i) the potential influence of steric hindrance imposed by the substituents located at BODIPY positions 1 and 3 (methyl groups in this case); (ii) possible competition from nucleophilic substitution at the BODIPY boron; (iii) compatibility with highly reactive functionalities such as primary alkyl halides or formyl groups; and (iv) the impact of the functionalization on the dye's photophysics.

To our pleasure, the isolated yields reached, which range from 84% for compound **5g** (derivatization with highly nucleophilic propargylamine) to 44% for **5b** (derivatization with highly unstable 2-bromoethanol), demonstrate the workability of the methodology with different NuHs, including highly reactive/unstable ones. These yields are comparable to those previously reported for analogous S_N1 transformations involving (4,4-dicyanoBODIPY-3-yl)methyl cations,[13] and are significantly influenced by the ability of the introduced moiety to act as a leaving group (nucleofuge), or undergo further transformation due to the presence of additional reactive groups.

BODIPYs. To evaluate the scope of the proposed methodology with respect to the starting BODIPY scaffolds, we selected a focused set of accessible 2,6-unsubstituted dyes featuring distinct electronic and steric profiles, using BnOH as the model

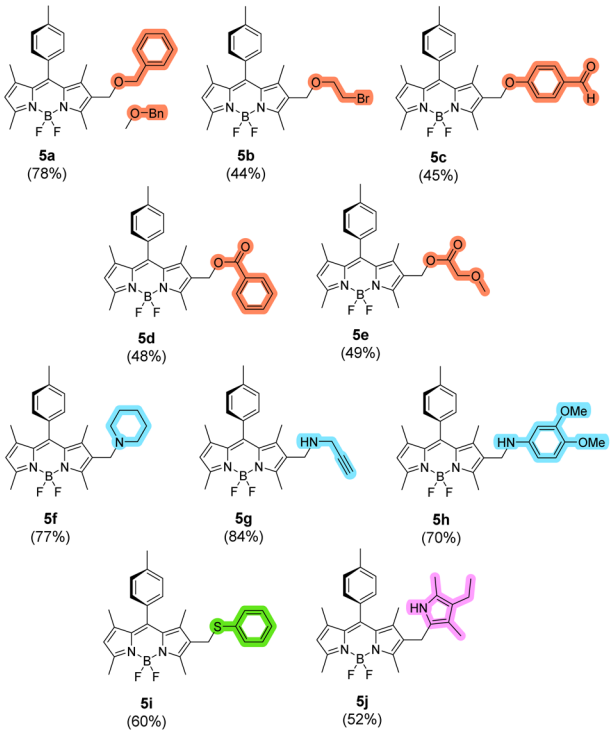

Fig. 1 Workable diversification of compound **1** *via* enabler **2** (see Scheme 2) with selected NuH species: benzyl alcohol (→ **5a**), 2-bromoethanol (**5b**), 4-hydroxybenzaldehyde (**5c**), benzoic acid (**5d**), methoxyacetic acid (**5e**), piperidine (**5f**), propargylamine (**5g**), 3,4-dimethoxyaniline (**5h**), thiophenol (**5i**), and 2,4-dimethyl-3-ethylpyrrole (**5j**). The introduced methylene-spaced Nu moiety is highlighted in red (O-nucleophiles), blue (N-nucleophiles), green (S-nucleophile), and pink (C-nucleophile). Isolated chemical yields from **2** are indicated in parentheses. See the SI for full experimental details.

nucleophile. For comparative purposes, the selected set includes the previously studied *meso*-arylated BODIPY **1**, the related *meso*-unsubstituted BODIPY **6** (the commercial PM505 laser dye) and *meso*-methylated BODIPY **7** (the commercial PM546 laser dye), as well as the π-extended BODIPY **8** (see Fig. 2), the later obtained by Knoevenagel-type double condensation of **1** with 4-fluorobenzaldehyde under microwave-assisted conditions (48%; see the SI for details).

As shown in Fig. 2, the corresponding (dimethylamino)methylated enablers (**2** and **9–11**) were successfully obtained in all cases with comparable isolated yields, ranging from 70% for **11** to 85% for **9**. This is particularly noteworthy considering the significantly varying reactivity of the selected BODIPYs toward S_EAr (**1** < **6** < **7** < **8**), driven by the electronic effects of their substituents. These results can be attributed to the high electrophilic character of Eschenmoser's salt. Remarkably, even in the case of **7**, where competitive Mannich-type condensation at the highly-reactive, enolizable-like *meso*-methyl position could occur,[15d] preferential mono-S_EAr at the BODIPY 2-position was observed, confirming the retention of regioselectivity and chemoselectivity across the series.

Moreover, all the synthesized enablers underwent nucleophilic substitution with BnOH at the expected methylene position with similarly high yields (78–84%), with the exception of π-extended **11** that gave **14** with lower yield (51%) (Fig. 2). Nonetheless, the

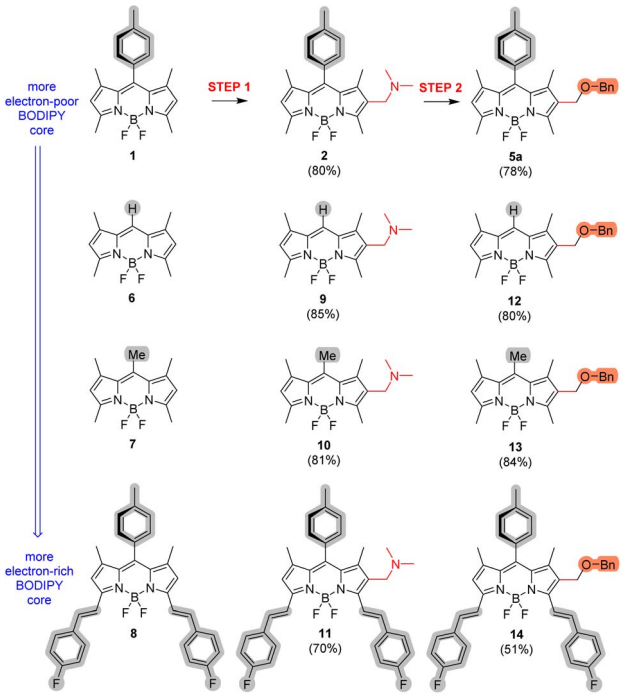

Fig. 2 Workable diversification of selected BODIPYs **1** and **6–8** with benzyl alcohol (BnOH) *via* (dimethylamino)methylation (step 1) and subsequent, activated nucleophilic substitution (step 2) (see Scheme 2). See the SI for full experimental details.

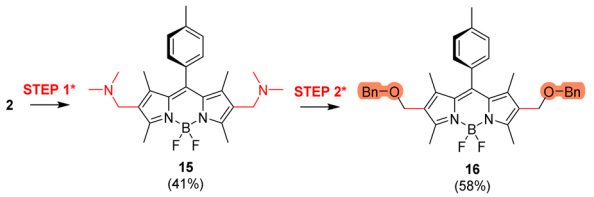

Scheme 3 Workable double functionalization of BODIPY **1** with benzyl alcohol (BnOH) *via* (dimethylamino)methylation of **1**-derived **2** (step 1*) and subsequent activated double nucleophilic substitution (step 2*). Experimental conditions were identical to those previously used for steps 1 and 2 (see Scheme 1), with only stoichiometric adjustment of the reagents in the case of step 2*. See the SI for full experimental details.

straightforward synthesis of compound **14** from π-extended BODIPY **8** *via* enabler **11** demonstrates the applicability of our method for the late-stage functionalization of valuable 3,5-bis(styrylated) red-emitting BODIPYs with nucleophiles (Fig. 2).

Regarding valuable methylene-spaced amination at the BODIPY 2-position (*e.g.*, compounds **2**, **5f–h**, and **9–11** in Fig. 1 and 2), the newly developed method provides an efficient alternative to the conventional Vilsmeier–Haack formylation followed by reductive amination.[19] In contrast to this traditional route, which requires properly substituted F-BODIPY precursors, particularly 3-aryl-F-BODIPYs, to minimize side-product formation during formylation,[15] the new strategy straightforwardly operates on a broad scope of starting materials.

Double functionalization. To assess the potential extension of the methodology to the preparation of photonically-valuable symmetric BODIPYs,[20] once again we selected BODIPY **1** and BnOH for comparisons (Scheme 1). Gratifyingly, the reaction of **1**-derived **2** with Eschenmoser's salt in the same conditions as the ones used to obtain 2 from 1, led to the expected "double" enabler **15** (41% yield). Then, after reaction of **15** with double stoichiometric amount of BnOH—while maintaining all other reaction conditions unchanged—we successfully obtained the expected final, doubly substituted symmetric BODIPY **16** (58% yield) (Scheme 3).

Photophysical impact

To assess the photophysical impact of the developed BODIPY-functionalization method, we characterized all functionalized dyes—including the (dimethylamino)methylated enablers—and the corresponding starting materials in diluted solutions of organic solvents with varying polarity, specifically toluene, chloroform, and acetonitrile (ACN) (see the SI for full experimental details). This allowed us to investigate for potential solvent-dependent processes such as fluorescence-damping intramolecular charge transfer (ICT) or fluorescence-quenching photoinduced electron transfer (PET). The main photophysical data are detailed in the SI (see Tables S1, S3 and S4 in the SI).

As shown in those tables, the developed methylene-spaced functionalization of BODIPYs exerts minimal influence on their light-absorption properties. This outcome was expected, as the methylene spacer likely prevents strong electronic coupling between the chromophoric BODIPY core and the appended n- or π-type substituents. Indeed, all the analysed BODIPY derivatives display sharp and intense absorption bands, with molar extinction coefficients (ε) ranging from 70 000 to 90 000 M^{-1} cm^{-1} (*e.g.*, see absorption spectra of

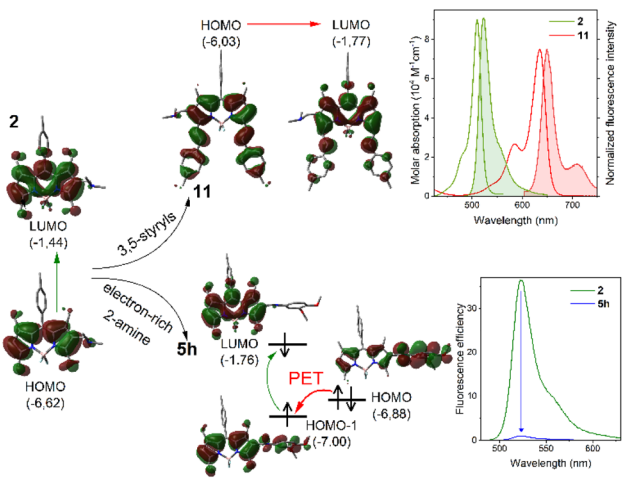

Fig. 3 Computed (CAM-B3LYP/6-311g*) electronic contour maps and energy levels (in eV) of the key frontier molecular orbitals (FMOs) for amine-based BODIPY **2**, and related compounds **11** (bearing either styryls instead of methyls at 3/5) and **5h** (bearing electron-richer amine (aniline) moiety), supporting feasibility for fluorescence-quenching reductive PET in the case of **5h**. The absorption and fluorescence (shaded) spectra of **2** and **11** (top right, in toluene) and the fluorescence spectra of **2** and **5h** (bottom right, in acetonitrile) are included for comparison purposes. For computed FMOs for related, PET-enabling **5j** see Fig. S1 in the SI. See the SI for full experimental details.

representative green-emitting **2** and red-emitting **11** in Fig. 3). Moreover, the absorption maxima match with that of the corresponding starting BODIPY dye (~500–515 nm for the derivatives of **1**, **6**, and **7**, and ~630 nm for those derived from π-extended **8**; *e.g.*, see the absorption spectra of **2** and **11** in Fig. 3).

Functionalization with O- and S-nucleophiles generally maintains—or even slightly enhances—fluorescence quantum yields, regardless of solvent polarity (*e.g.*, compare **1** with **5a–e**, **5i–j** and **16**; **6** with **12**; **7** with **13**; and **8** with **14**; in Fig. 4 and Table S1 in the SI).

In contrast, substitution with N-based moieties leads to pronounced variations in fluorescence efficiency that are both structure- and solvent-dependent (*e.g.*, compare **1** with **2** and **5h**; **6** with **9**; **7** with **10**; and **8** with **11** in Fig. 4). Thus, the fluorescence of the derivatives bearing electron-rich tertiary-amine moieties (**2**, **5f**, **15** and **9–11**) clearly drops in polar solvents, where it becomes almost negligible (see Tables S1, S3 and S4 in the SI). This trend is softened when electron-poorer secondary-amine moieties are involved instead (*e.g.*, compare **5f** with **5g** in Table S1 in the SI), or when the electron richness of the BODIPY core is enhanced (*e.g.*, compare **2** with **11** in Fig. 4). As above mentioned, all this is consistent with polar-solvent promoted photoinduced ICT, taking place through the space from the electron-rich amino group to the electron-poor BODIPY core.[21]

Regarding fluorescence, the emission maxima wavelengths of the functionalized dyes are largely preserved relative to their respective starting materials (see Tables S1, S3 and S4 in SI). However, fluorescence intensity is highly dependent on the electronic nature of the introduced functionality (Fig. 4). The measured electrochemical properties of representative compounds (see the SI for full experimental details) further support the ICT pathway in those dyes functionalized with sufficiently electron-donating amine-based moieties (Fig. S2 in the SI). Thus, ICT-enabling **2** and **15**, which bear tertiary alkyl amine groups, exhibit lower oxidation potentials (1.13 and 1.21 V, respectively) compared to related **5a** (oxidation potential = 1.38 V), the latter bearing alcohol-based moiety and exhibiting no evidence of fluorescence-damping ICT.

Conversely, involving an electron-rich arenamine-based moiety strongly affects the fluorescence capability of the dye, as observed in the case of **5h** (see Fig. 4), where almost null fluorescence is observed, even in the case of apolar toluene as the solvent. In this particular case, the strong electron-donating capability of the arenamine system, increased by the attached methoxyl groups, promotes fluorescence-quenching by PET from the electron-rich π-conjugated arenamine moiety to the electron-poor BODIPY core, as supported computationally (Fig. 3). Thus, light excitation is computed to promote electronic transition from HOMO−1 to LUMO, both localized at the BODIPY core, enabling thermodynamically-feasible reductive PET from the HOMO (located at the arenamine moiety) to the semivacant HOMO−1, which becomes fully occupied and prevents radiative deactivation by electronic transition from the semivacant LUMO (see Fig. 3). Indeed, compound **5h** exhibits the lowest oxidation potential (0.78 V) among all the functionalized dyes analysed in this study, supporting its high propensity to undergo electron transfer processes (see Fig. S2 in the SI).

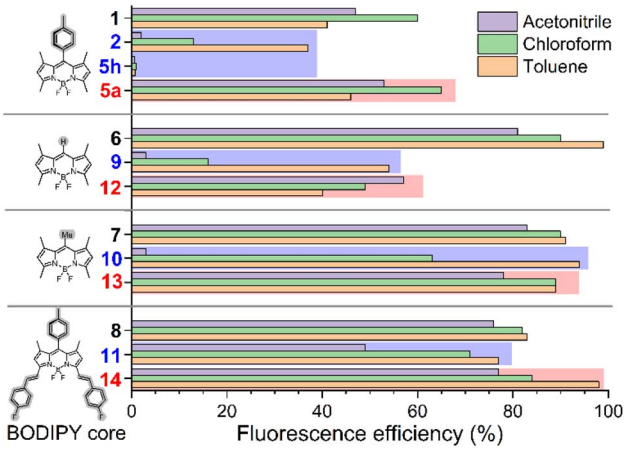

Fig. 4 Representative structure- and solvent-dependent variations in fluorescence efficiency for selected BODIPYs (**1** and **6–8**; non-shaded data) upon methylene-spacer based functionalization with N-nucleophile (**2**, **5h** and **9–11**; blue-shaded data) and O-nucleophile (**5a** and **12–14**; red-shaded data) moieties at BODIPY 2-position. Data selected from Tables S1, S3 and S4 in the SI.

A related fluorescence-quenching PET process, although less thermodynamically favoured, is also observed for compound **5j**, which features an electron-rich 2-pyrrolyl moiety (see Fig. S1 in the SI).

All these results demonstrate that the developed functionalization methodology allows diversification of BODIPY dyes with a broad variety of NuHs without significantly affecting the outstanding light absorption capability of the starting dyes, which makes it ideal for developing dyed materials for photonic applications based on light absorption. Fluorescence maxima are also maintained, however, the starting BODIPY core and introduced nucleophilic moiety must be carefully selected when highly-brilliant final materials are targeted, and the use of electron-rich tertiary amines should be avoided in this case.

Showcasing some applications

The synthetic accessibility and selectable photophysical behaviour—achieved through the induction of ICT or PET processes—make the new BODIPY functionalization methodology ideally suited for the development of photonic applications in which designing ICT/PET-based fluorescence variations or the straightforward incorporation of additional functions is essential. To demonstrate this potential, we selected two representative application areas: ICT-based BODIPY probes,[22] specifically fluorescent pH indicators and fluorogenic acidotropic bioprobes, and water-soluble BODIPY-based laser dyes.[23,3c]

ICT-based probes. As previously mentioned, employing amines as NuHs in the newly developed BODIPY-functionalization methodology impacts the fluorescence behaviour of the final, functionalized dye by enabling ICT, particularly when secondary alkyl amines are used as nucleophiles. This fact, combined with the Brønsted basicity of benzyl-like tertiary amines ($pK_b \approx 4.5$), makes the readily accessible 2-[(dialkylamino)methyl]BODIPYs ideal candidates for ICT-based

pH sensing. Thus, upon protonation of the tertiary amine group to form the corresponding ammonium salt, the ICT process responsible for fluorescence damping should be disrupted, resulting in a significant, and therefore easily measurable, fluorescence enhancement.

To explore this potential, we selected compounds **2** and **5f** (see Scheme 2 and Fig. 2), both featuring tertiary alkyl amine moieties, and monitored the changes in the fluorescence spectra in ethanol solution (4.0 μM) upon incremental addition of *p*-toluenesulfonic acid (TsOH). Gratifyingly, fluorescence intensity increased progressively with acid concentration, especially after the addition of 4 equivalents of TsOH (fluorescence quantum yield ≈ 0.05), reaching a plateau at approximately 7 equivalents (fluorescent quantum yield ≈ 0.65 for **5f**, and ≈ 0.46 for **2**) (see Fig. 5 for **5f**, and S3 in the SI for **2**). These results confirm that protonation of the amine effectively suppresses ICT, thereby significantly enhancing fluorescence efficiency. Notably, the fluorescent brightness of the protonated species in ethanol exceeds that of the non-protonated species in apolar solvents, and surpasses values reported for structurally related BODIPY-based fluorescent pH indicators featuring (dialkylamino)methyl substitution at the BODIPY 3-position instead of the BODIPY 2-position.[13]

This pH-dependent fluorescence response is also evident in the fluorescence lifetimes, making possible advantageous lifetime-based pH sensing approaches.[24] For instance, compound **5f** shows a biexponential fluorescence decay in ethanol in its non-protonated form, with a dominant short lifetime component (~0.15 ns). Upon protonation, the decay becomes monoexponential with a markedly longer lifetime of 3.20 ns—a 21-fold increase (see Fig. S4 in the SI).

The significant enhancement of fluorescence observed in 2-(dialkylamino)methylated BODIPYs upon protonation, combined with their straightforward synthesis, actuation pH range (~4.0–5.0), expected biocompatibility and cell-membrane permeability, makes them ideal candidates as highly sensitive fluorogenic acidotropic lysosomal probes (Fig. 5).

Fluorogenic probes are especially valuable for bioimaging because they allow high-contrast visualization by minimizing background fluorescence in non-target regions.[25] This "signal-on" behaviour not only improves imaging sensitivity but also simplifies experimental protocols by reducing the need for wash steps. In the context of live-cell imaging, where non-invasive, selective, and responsive indicators are key, fluorogenic probes capable of activation under specific physiological stimuli—such as pH shifts—are of particular interest for tracking intracellular events in real time.[25]

Particularly, cell-permeant pH-activatable (fluorogenic) acidotropic lysosomal probes (specifically marketed LysoSensors™) have been highlighted as valuable tools for investigating aberrant pH variations in lysosomes and other organelles, as well as alterations in lysosomal function or trafficking that are associated with major pathologies such as cancer, cystic fibrosis, and related diseases.[26,27] However, pH-LysoSensor™ probes are limited to a small number of dyes, and their fluorescence efficiency in the protonated (fluorescent) state—and likely their long-term photostability—is significantly

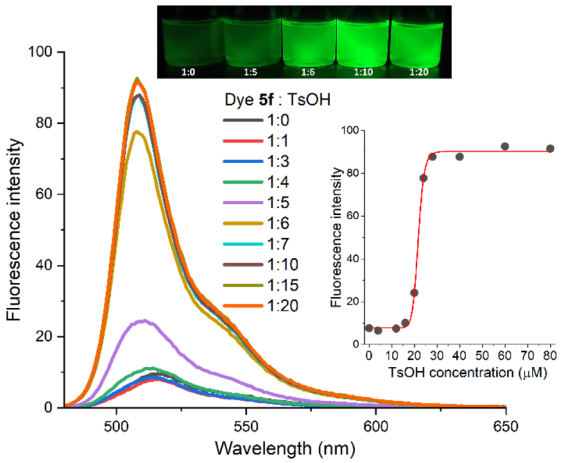

Fig. 5 Variation of the fluorescence of compound **5f** (4 μM in ethanol) upon incremental addition of TsOH (molar ratios from 1 : 0 to 1 : 20). Naked-eye brightness (top) and fluorescence spectra (bottom left). The dependence of the fluorescence intensity at 508 nm on proton concentration (bottom right) is also shown, highlighting pH sensitivity around apparent pH ≈ 4.5. See the SI for full experimental details.

lower than that of the widely used LysoTracker™ probes, which are based on highly bright and photostable BODIPY fluorophores.[26] Nevertheless, LysoTrackers™ do not exhibit marked fluorescence enhancement under acidic conditions,[26] limiting their usefulness as ratiometric or pH-sensitive indicators. Consequently, the low fluorescence output of existing fluorogenic acidotropic sensors can pose a drawback in fluorescence-based applications, such as quantifying lysosomal number or tracking pH variations *via* flow cytometry or fluorometric analysis.[26,28] In this context, the herein developed readily-accessible 2-(dialkylamino)methyl BODIPYs could surpass the performance of the commercially available LysoSensor™ probes.

To evaluate this potential, we selected compounds **2** and **5f** and employed wild-type mouse embryonic fibroblasts (MEFs) as a cellular model. Computational prediction of pharmacokinetic parameters using the freely available SwissADME web tool[29] indicated good permeability and biocompatibility profiles for both compounds. Encouragingly, both **2** and **5f** efficiently stained living MEFs (see the SI for full experimental details), enabling fluorescence bioimaging of lysosomes with high specificity, as confirmed by co-localization with LysoTracker™ Red (pearson's coefficients > 0.6) (see Fig. S5 in the SI). This result supports pH-activatable fluorescence probing of lysosomes, as the selected dyes are poorly fluorescent under non-acidic conditions (*e.g.*, see Fig. 5 for **5f**).

To assess the superior behaviour of our fluorogenic acidotropic probes, we compared the fluorescence brightness of MEFs treated in parallel and under nearly identical conditions with commercial LysoTracker™ Green,[26] and with compounds **2** and **5f**. LysoTracker™ Green was selected due to its close structural and functional, biophotonic similarity to **2** and **5f**: all three are highly bright, green-fluorescent BODIPY-based probes that exhibit comparable absorption and emission properties, and that accumulate specifically in lysosomes *via* a pendant tertiary alkyl amine that becomes protonated in the acidic

lysosomal environment. However, as mentioned above, the fluorescence of LysoTracker™ Green is nearly pH-independent.

Satisfactorily, significantly less excitation laser power was required to achieve comparable imaging quality in the case of compound **2**—and particularly compound **5f**—when compared to LysoTracker™ Green (see Fig. 6, and S6 in the SI).

Since fluorogenic acidotropic LysoSensors™ are significantly less fluorescent than LysoTrackers™, as mentioned above, all these results clearly demonstrate the higher performance of our 2-(dialkylamino)methyl BODIPYs as fluorogenic acidotropic lysosomal probes. Moreover, they highlight the potential of the newly developed BODIPY functionalization methodology to expand the current toolbox of acidotropic lysosomal sensors by enabling rapid access to advanced and structurally diverse probes, including valuable pH-activatable sensors operating in the biologically relevant red-to-NIR spectral region.[30]

Water-soluble laser dyes. The thermo-optic properties of the gain medium solvent, together with dye flow dynamics, are key parameters governing the maximum repetition rate of dye lasers.[31] Although water exhibits superior thermo-optic performance compared to alcoholic solvents, its use is often restricted by the limited solubility of many hydrophobic laser dyes, where the resulting formation of non-emissive aggregates reduces lasing efficiency and limits their applicability in water-based systems.[31] This limitation is particularly pronounced for the well-known BODIPY laser dyes,[32] which, despite their excellent fluorescence and photostability, display poor aqueous solubility. Given the central role of BODIPYs among modern laser dyes, the development of aqueous-compatible laser dyes remains a major objective in advancing dye laser technology.[31f,g,3c]

In this context, we hypothesized that the straightforward generation of BODIPYs functionalized with highly hydrophilic groups, enabled by the methodology described herein, could offer a practical route to impart water solubility to otherwise hydrophobic 2/6-unsubstituted BODIPY dyes, thereby enabling their use in aqueous laser operation.

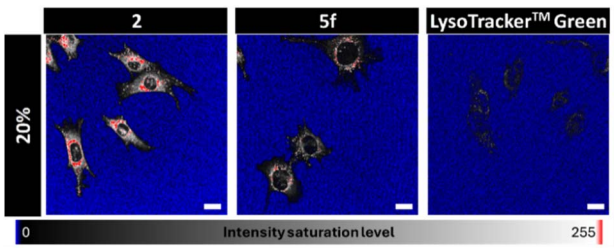

Fig. 6 Representative confocal laser scanning microscopy images of MEF cells acquired at a software setting of 20% laser power (corresponding to 274 μW power output), and represented in an 8-bit grayscale and pseudo-coloured using the LUT intensity saturation indicator. In this colour scale, fully saturated pixels (intensity = 255) are rendered red, and the darkest pixels (intensity = 0) are blue; intermediate intensities remain on a grayscale gradient. This colour scheme highlights overexposed regions in red and under-exposed/background areas in blue, allowing to compare signal distribution and saturation across samples for **2**, **5f** and LysoTracker™ Green when imaged at the same laser power. λ_{exc} = 488 nm and λ_{em} = 525 ± 25 nm. Scale bars are 20 μm. See the SI for full experimental details.

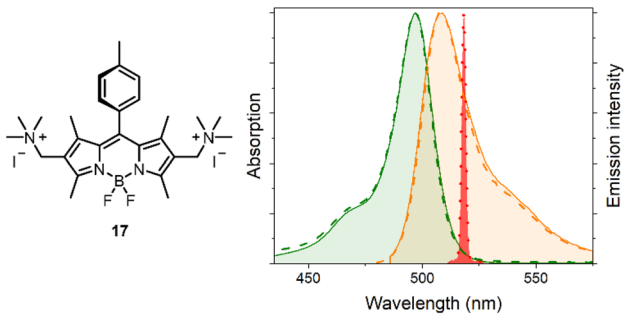

Fig. 7 Molecular structure of the newly developed water-operable laser dye **17**, shown alongside its normalized absorption (green-shaded), fluorescence (orange-shaded), and laser emission spectra (sharp red-shaded band with dotted line) recorded in pure water at high dye concentration (dye concentration = 0.2 mM). For comparison, the corresponding absorption and fluorescence spectra measured at dilute concentration (2 μM, dashed lines) in pure water are also included. See the SI for full experimental details.

To test this hypothesis, we selected the trimethylammonium-functionalized BODIPY **3**, along with the related difunctionalized dye **17** (Fig. 7), which was expected to exhibit improved aqueous solubility due to the presence of two ammonium groups. Compound **17** was prepared by quantitative methylation of the two amino groups of precursor **15** using methyl iodide under standard conditions.

The water solubility of **3** and **17** was experimentally evaluated, along with their photophysical behaviour in pure water. Both dyes were found to be highly soluble and fully stable in water—particularly the doubly and symmetrically substituted dye **17**, for which dye concentrations up to 0.2 mM could be achieved in pure water. Notably, no signs of aggregation were photophysically detected, even at the highest tested concentrations, as evidenced by the excellent overlap of the absorption and fluorescence spectra with those recorded at 100-fold lower concentrations (*e.g.*, see Fig. 7 for **17**). Importantly, the photophysical signatures recorded in pure water—such as a fluorescence quantum yield of approximately 0.50 for dye **17** (see Table S2 in the SI)—are comparable to those of the corresponding BODIPY precursor (*e.g.*, precursor **1** in the case of **17**) in organic solvents.

Remarkably, the high solubility, stability, and fluorescence of dye **17** in pure water enabled the recording of its laser emission in pure water. Thus, upon laser excitation of **17** in water, sharp and intense laser emission at 518 nm was observed (Fig. 7) with a lasing efficiency of 32%. This efficiency is comparable to that typically achieved by hydrophobic BODIPY laser dyes in organic solvents,[33] clearly demonstrating the potential of the newly developed BODIPY functionalization methodology for advancing valuable organic laser dyes operating efficiently in pure water.

Conclusions

In summary, we have developed a novel and broadly applicable strategy for the diversification of common and readily accessible BODIPY dyes with nucleophiles, employing the corresponding 2-(dimethylamino)methyl-substituted dyes as stable,

bench-accessible electrophilic intermediates. This platform enables efficient functionalization with a wide range of neutral protic nucleophiles under mild conditions. The methodology addresses longstanding limitations of related methylene-spacer based post-functionalization strategies, such as poor intermediate stability, narrow nucleophile and substrate scope, and reliance on hazardous or costly reagents.

The developed new BODIPY post-functionalization method combines synthetic simplicity—relying on widely available 2-unsubstituted BODIPYs and relatively inexpensive commercial reagents—with operational convenience and potential scalability. Notably, its compatibility with 3,5-dimethyl BODIPY derivatives retains access to valuable red-to-NIR emissive dyes through well-established Knoevenagel-type double-condensation strategy for BODIPY spectral red-shifting.

Crucially, the method enables the controlled installation of diverse nucleophilic moieties—including those bearing reactive functionalities—across a broad structural space, while preserving the intrinsic absorption properties of the parent BODIPY core. Fluorescence efficiency is also maintained when the introduced groups are carefully selected, avoiding quenching elements such as electron-rich tertiary amines.

The demonstrated ability to generate a wide array of BODIPY dyes with tailored substitution patterns and selectable photophysical behaviour opens new avenues for the design of functional, fully organic molecular photonic tools. This potential is exemplified by the successful development of advanced fluorescent pH indicators, water-soluble laser dyes, and fluorogenic acidotropic bioprobes.

Altogether, the post-functionalization methodology presented here significantly expands the synthetic toolbox of BODIPY chemistry, and establishes a versatile foundation for future innovation in the fields of organic photonics and chiroptics.

Author contributions

S. d. l. M., conceptualization; S. d. l. M. and B. L. M. supervision; S. S.-B., C. M. and A. A., investigation (synthetic development); F. M., investigation (structural characterization); N. C. and J. B., investigation ((photo)physical behaviour); D. V. G. and I. L.-M., investigation (live-cell imaging validation); B. L. M., S. d. l. M., J. B., F. M. and I. L.-M., writing (review and editing); S. d. l. M. and B. L. M., writing (original draft).

Conflicts of interest

There are no conflicts to declare.

Data availability

The data supporting this article have been included as part of the supplementary information (SI). Supplementary information: general methods and equipment, synthetic procedures and characterization, NMR spectra of new compounds, as well as additional figures concerning (photo)physical and (bio)photonical behaviours. See DOI: https://doi.org/10.1039/d5sc08677a.

Acknowledgements

S. d. l. M. and B. L. M. acknowledge project PID2024-157648-NB-C21 (granted by MICIU/AEI/10.13039/501100011033 and FEDER, UE). J. B. acknowledges projects PID2024-157648-NB-C22 (granted by MICIU/AEI/10.13039/501100011033 and FEDER, UE) and IT2001-26 (granted by Basque Government). S. S.-B., C. M. and D. V. G. acknowledge UCM and Banco Santander for their pre-doctoral contracts (CT58/21-CT59/21, CT25/24 and CT58/21-CT59/21, respectively).

Notes and references

1 (*a*) X. Hu, Z. Fang, C. Zhu, Y. Yang, Z. Yang and W. Huang, *Adv. Funct. Mater.*, 2024, **34**, 2401325; (*b*) X. Hu, Z. Fang, C. Zhu, Y. Yang, Z. Yang and W. Huang, *Adv. Funct. Mater.*, 2024, **34**, 2401325; (*c*) P. Stachelek, S. Serrano-Buitrago, B. L. Maroto, R. Pal and S. de la Moya, *ACS Appl. Mater. Interfaces*, 2024, **16**, 67246–67254; (*d*) J. Chen, Q. Sha, M. U. Rehman, M. Wu, Z. Hu and F. Wu, *ACS Appl. Nano Mater.*, 2024, **7**, 23122–23132; (*e*) A. Garcia-Sampedro, A. Prieto-Castañeda, A. R. Agarrabeitia, J. Bañuelos, I. Garcia-Moreno, A. Villanueva, S. de la Moya, M. J. Ortiz and P. Acedo, *J. Mater. Chem. B*, 2024, **12**, 7618–7625; (*f*) H. Li, X. Xu, R. Guan, A. Movsesyan, Z. Lu, Q. Xu, Z. Jiang, Y. Yang, M. Khan, J. Wen, H. Wu, S. de la Moya, G. Markovich, H. Hu, Z. Wang, Q. Guo, T. Yi, A. O. Govorov, Z. Tang and X. Lan, *Nat. Commun.*, 2024, **15**, 4846; (*g*) L. Gutierrez-Galvez, E. Enebral-Romero, M. A. Valle Amores, C. Pina Coronado, I. Torres, D. Lopez-Diego, M. Luna, A. Fraile, F. Zamora, J. Aleman, J. Álvarez, M. J. Capitán, E. Lorenzo and T. García-Mendiola, *Nanoscale*, 2025, **17**, 8126–8140; (*h*) Z. Chen, Y. Zhou, L. Li, W. Ma, Y. Li and Z. Yang, *Small*, 2025, **21**, 2411787; (*i*) N. Lin and T. Mani, *J. Am. Chem. Soc.*, 2025, **147**, 7187–7190; (*j*) F. Wang, F. Tan, W. Zhao, S. Zhou, Q. Xu, L. Kan, L. Zhu, P. Gu and J. Lu, *Angew. Chem., Int. Ed.*, 2025, **64**, e202425017.

2 (*a*) A. Loudet and K. Burgess, *Chem. Rev.*, 2007, **107**, 4891–4932; (*b*) R. Ziessel, G. Ulrich and A. Harriman, *New J. Chem.*, 2007, **31**, 496–501; (*c*) G. Ulrich, R. Ziessel and A. Harriman, *Angew. Chem., Int. Ed.*, 2008, **47**, 1184–1201; (*d*) H. Lu, J. Mack, Y. Yang and Z. Shen, *Chem. Soc. Rev.*, 2014, **43**, 4778–4823; (*e*) J. Zhao, K. Xu, W. Yang, Z. Wang and F. Zhong, *Chem. Soc. Rev.*, 2015, **44**, 8904–8939; (*f*) N. Boens, B. Verbelen and W. Dehaen, *Eur. J. Org Chem.*, 2015, **2015**, 6577–6595; (*g*) V. Lakshmi, M. R. Rao and M. Ravikanth, *Org. Biomol. Chem.*, 2015, **13**, 2501–2517; (*h*) L. Jean-Gerard, W. Vasseur, F. Scherninski and B. Andrioletti, *Chem. Commun.*, 2018, **54**, 12914–12929; (*i*) E. Bodio and C. Goze, *Dyes Pigm.*, 2019, **160**, 700–710; (*j*) R. G. Clarke and M. J. Hall, *Adv. Heterocycl. Chem.*, 2019, **128**, 181–261; (*k*) N. Boens, B. Verbelen, M. J. Ortiz, L. Jiao and W. Dehaen, *Coord. Chem. Rev.*, 2019, **399**, 213024; (*l*) N. A. Bumagina, E. V. Antina, A. A. Ksenofontov, L. A. Antina, A. A. Kalyagin and M. B. Berezin, *Coord. Chem. Rev.*, 2022, **469**, 214684; (*m*) R. L. Gapare and A. Thompson, *Chem. Commun.*, 2022, **58**, 7351–7359; (*n*)

D. Alvarez-Gutierrez, D. Sampedro, M. C. Jimenez, R. Perez-Ruiz and A. C. S. Appl, *Opt. Mater.*, 2024, **2**, 1780–1789; (*o*) M. Bogomolec, M. Glavas and I. Skoric, *Molecules*, 2024, **29**, 5157; (*p*) J. G. Becerra-Gonzalez, E. Peña-Cabrera and J. L. Belmonte-Vazquez, *Tetrahedron*, 2024, **168**, 134334; (*q*) R. Segovia-Perez, M. Ibarra-Rodriguez, B. M. Munoz-Flores and V. M. Jimenez-Perez, *Dyes Pigm.*, 2025, **239**, 112740; (*r*) A. S. Sherudillo, L. A. Antina and E. V. Antina, *Coord. Chem. Rev.*, 2025, **545**, 217030.

3 (*a*) C. S. Mahanta, V. Ravichandiran and S. P. Swain, *ACS Appl. Bio Mater.*, 2023, **6**, 2995–3018; (*b*) H.-B. Cheng, X. Cao, S. Zhang, K. Zhang, Y. Cheng, J. Wang, J. Zhao, L. Zhou, X.-J. Liang and J. Yoon, *Adv. Mater.*, 2023, **35**, 2207546; (*c*) C. Schad, C. Ray, C. Díaz-Norambuena, S. Serrano-Buitrago, F. Moreno, B. L. Maroto, I. García-Moreno, M. Muñoz-Úbeda, I. López-Montero, J. Bañuelos and S. de la Moya, *Chem. Sci.*, 2025, **16**, 8030–8039.

4 (*a*) Y. Ni and J. Wu, *Org. Biomol. Chem.*, 2014, **12**, 3774–3791; (*b*) T. Kowada, H. Maeda and K. Kikuchi, *Chem. Soc. Rev.*, 2015, **44**, 4953–4972; (*c*) S. Kolemen and E. U. Akkaya, *Coord. Chem. Rev.*, 2018, **354**, 121–134; (*d*) V.-N. Nguyen, J. Ha, M. Cho, H. Li, K. M. K. Swamy and J. Yoon, *Coord. Chem. Rev.*, 2021, **439**, 213936; (*e*) S. Samanta, K. Lai, F. Wu, Y. Liu, S. Cai, X. Yang, J. Qu and Z. Yang, *Chem. Soc. Rev.*, 2023, **52**, 7197–7726; (*f*) H. Ahmad, S. Muhammad, M. Mazhar, A. Farhan, M. S. Iqbal, H. Hiria, C. Yu, Y. Zhang and B. Guo, *Coord. Chem. Rev.*, 2025, **526**, 216383; (*g*) P. P. P. Kumar, S. Saxena and R. Joshi, *Colorants*, 2025, **4**, 13; (*h*) C. Kalarikkal and C. A. Swamy, *J. Mater. Chem. B*, 2025, **13**, 12831–12868.

5 (*a*) N. Boens, V. Leen and W. Dehaen, *Chem. Soc. Rev.*, 2012, **41**, 1130–1172; (*b*) H. N. Kim, W. X. Ren, J. S. Kim and J. Yoon, *Chem. Soc. Rev.*, 2012, **41**, 3210–3244; (*c*) Y. T. Nguyen, S. Shin, K. Kwon, N. Kim and S. W. Bae, *J. Chem. Res.*, 2023, **47**, 17475198231168961; (*d*) N. A. Bumagina and E. V. Antina, *Coord. Chem. Rev.*, 2024, **505**, 215688; (*e*) S. Routray, S. Acharya, L. Nayak, S. Pattnaik and R. Satapathy, *RSC Adv.*, 2025, **15**, 9910–9951.

6 J. Zhao, K. Xu, W. Yang, Z. Wang and F. Zhong, *Chem. Soc. Rev.*, 2015, **44**, 8904–8939.

7 (*a*) S. G. Awuah and Y. You, *RSC Adv.*, 2012, **2**, 11169–11183; (*b*) A. Kamkaew, S. H. Lim, H. B. Lee, L. V. Kiew, L. Y. Chung and K. Burgess, *Chem. Soc. Rev.*, 2013, **42**, 77–88; (*c*) C. S. Kue, S. Y. Ng, S. H. Voon, A. Kamkaew, L. Y. Chung, L. V. Kiew and H. B. Lee, *Photochem. Photobiol. Sci.*, 2018, **17**, 1691–1708; (*d*) A. Turksoy, D. Yildiz and E. U. Akkaya, *Coord. Chem. Rev.*, 2019, **379**, 47–64; (*e*) M. L. Agazzi, M. B. Ballatore, A. M. Durantini, E. N. Durantini and A. C. Tomé, *J. Photochem. Photobiol., C*, 2019, **40**, 21–48; (*f*) R. Prieto-Montero, A. Prieto-Castañeda, R. Sola-Llano, A. R. Agarrabeitia, D. García-Fresnadillo, I. López-Arbeloa, Á. Villanueva, M. J. Ortiz, S. de la Moya and V. Martínez-Martínez, *Photochem. Photobiol.*, 2020, **96**, 458–477; (*g*) X. Hu, Z. Fang, C. Zhu, Y. Yang, Z. Yang and W. Huang, *Adv. Funct. Mater.*, 2024, **34**, 2401325.

8 D. Alvarez-Gutierrez, D. Sampedro, M. C. Jimenez and R. Perez-Ruiz, *ACS Appl. Opt. Mater.*, 2024, **2**, 1780–1789.

9 (*a*) P. De Bonfils, L. Peault, P. Nun and V. Coeffard, *Eur. J. Org Chem.*, 2021, **2021**, 1809–1824; (*b*) P. Rana, N. Singh, P. Majumdar and S. P. Singh, *Coord. Chem. Rev.*, 2022, **470**, 214698; (*c*) D. Zhang, L. Liu, X. Zhang, J. Lu and X.-D. Jiang, *Resour. Chem. Mater.*, 2024, **3**, 103–122.

10 (*a*) H. Lu, J. Mack, T. Nyokong, N. Kobayashi and Z. Shen, *Coord. Chem. Rev.*, 2016, **318**, 1–15; (*b*) H. Tanaka, Y. Inoue and T. Mori, *ChemPhotoChem*, 2018, **2**, 386–402; (*c*) M. J. Hall and S. de la Moya, in *Circularly Polarized Luminescence of Isolated Small Organic Molecules*, ed. T. Mori, Springer, Singapore, 2020, pp. 117–150; (*d*) M. Ikeshita and T. Tsuno, *Phys. Chem. Chem. Phys.*, 2025, **27**, 17116–17129.

11 (*a*) A. Bessette and G. S. Hanan, *Chem. Soc. Rev.*, 2014, **43**, 3342–3400; (*b*) S. P. Singh and T. Gayathri, *Eur. J. Org Chem.*, 2014, **2014**, 4689–4707; (*c*) D. Ho, R. Ozdemir, H. Kim, T. Earmme, H. Usta and C. Kim, *ChemPlusChem*, 2019, **84**, 18–37; (*d*) M. Poddar and R. Misra, *Coord. Chem. Rev.*, 2020, **421**, 213462; (*e*) B. M. Squeo and M. Pasini, *Supramol. Chem.*, 2020, **32**, 56–70.

12 G. Ulrich, R. Ziessel and A. Haefele, *J. Org. Chem.*, 2012, **77**, 4298–4311.

13 A. Blázquez-Moraleja, L. Maierhofer, E. Mann, R. Prieto-Montero, A. Oliden-Sánchez, L. Celada, V. Martínez-Martínez, M.-D. Chiara and J. L. Chiara, *Org. Chem. Front.*, 2022, **9**, 5774–5789.

14 (*a*) H. Lu, J. Mack, Y. Yang and Z. Shen, *Chem. Soc. Rev.*, 2014, **43**, 4778–4823; (*b*) J. Jiménez, C. Díaz-Norambuena, S. Serrano, S. C. Ma, F. Moreno, B. L. Maroto, J. Bañuelos, G. Muller and S. de la Moya, *Chem. Commun.*, 2021, **57**, 5750–5753; (*c*) C. Kalarikkal and P. C. A. Swamy, *J. Mater. Chem. B*, 2025, **13**, 12831–12868; (*d*) Y. Li, M. Jiang, M. Yan, J. Ye, Y. Li, W. Dehaen and S. Yin, *Coord. Chem. Rev.*, 2024, **506**, 215718.

15 (*a*) L. Jiao, C. Yu, J. Li, Z. Wang, M. Wu and E. Hao, *J. Org. Chem.*, 2009, **74**, 7525–7528; (*b*) C. Yu, L. Jiao, H. Yin, J. Zhou, W. Pang, Y. Wu, Z. Wang, G. Yang and E. Hao, *Eur. J. Org Chem.*, 2011, **2011**, 5460–5468; (*c*) D. E. Ramirez-Ornelas, E. Alvarado-Martinez, J. Bañuelos, I. Lopez Arbeloa, T. Arbeloa, H. M. Mora-Montes, L. A. Perez-Garcia and E. Pena-Cabrera, *J. Org. Chem.*, 2016, **81**, 2888–2898; (*d*) E. Palao-Utiel, L. Montalvillo-Jimenez, I. Esnal, R. Prieto-Montero, A. R. Agarrabeitia, I. Garcia-Moreno, J. Bañuelos, I. Lopez-Arbeloa, S. de la Moya and M. J. Ortiz, *Dyes Pigm.*, 2017, **141**, 286–298.

16 (*a*) Z.-X. Wang and B. Yang, *Org. Biomol. Chem.*, 2020, **18**, 1057–1072; (*b*) J. Templ and M. Schnürch, *Chem. – Eur. J.*, 2024, **30**, e202400675.

17 A. Cui, X. Peng, J. Fan, X. Chen, Y. Wu and B. Guo, *J. Photochem. Photobiol., A*, 2007, **186**, 85–92.

18 E. Palao, S. de la Moya, A. R. Agarrabeitia, I. Esnal, J. Bañuelos, I. López-Arbeloa and M. J. Ortiz, *Org. Lett.*, 2014, **16**, 4364–4367.

19 (*a*) X. Gu, C. Liu, Y.-C. Zhu and Y.-Z. Zhu, *Tetrahedron Lett.*, 2011, **52**, 5000–5003; (*b*) C. Zhao, Y. Zhang, P. Feng and J. Cao, *Dalton Trans.*, 2012, **41**, 831–838; (*c*) L. Wang, Y. Xiao, W. Tian and L. Deng, *J. Am. Chem. Soc.*, 2013, **135**,

2903–2906; (*d*) C. Zhao, X. Li and J. Zhang, *Inorg. Chim. Acta*, 2014, **412**, 32–37; (*e*) H. Wang, Y. Wu, Y. Shi, P. Tao, X. Fan, X. Su and G.-C. Kuang, *Chem. – Eur. J.*, 2015, **21**, 3219–3223; (*f*) Z. Xu, Y. Huang, Y. Cao, T. Jin, K. A. Miller, A. L. Kaledin, D. G. Musaev, T. Lian and E. Egap, *J. Chem. Phys.*, 2020, **153**, 154201; (*g*) A. M. Gómez, A. H. G. David, A. G. Campaña, J. M. Cuerva, L. Díaz-Casado, C. Uriel, A. Oliden-Sánchez, J. Bañuelos, I. García-Moreno, L. Infantes, C. M. Cruz, J. T. Chambi and J. C. López, *J. Org. Chem.*, 2024, **89**, 18522–18528.

20 (*a*) I. García-Moreno, L. Wang, Á. Costela, J. Bañuelos, I. López Arbeloa and Y. Xiao, *ChemPhysChem*, 2012, **13**, 3923–3931; (*b*) E. M. Sánchez-Carnerero, F. Moreno, B. L. Maroto, A. R. Agarrabeitia, M. J. Ortiz, B. G. Vo, G. Muller and S. de la Moya, *J. Am. Chem. Soc.*, 2014, **136**, 3346–3349; (*c*) E. Avellanal-Zaballa, J. Ventura, L. Gartzia-Rivero, J. Bañuelos, I. García-Moreno, C. Uriel, A. M. Gómez and J. C. López, *Chem. – Eur. J.*, 2019, **25**, 14959–14971.

21 (*a*) R. B. Alnoman, P. Stachelek, J. G. Knight, A. Harriman and P. G. Waddell, *Org. Biomol. Chem.*, 2017, **15**, 7643–76513; (*b*) F.-Z. Li, Z. Wu, C. Lin, Q. Wang and G.-C. Kuang, *Results Chem.*, 2022, **4**, 1000384.

22 Y. Wu, C. Ge, Y. Zhang, Y. Wang and D. Zhang, *Front. Chem.*, 2023, **11**, 1304531.

23 S. Sinha, A. K. Ray, S. Kundu, S. Sasikumar and K. Dasgupta, *Appl. Phys. B*, 2002, **75**, 85.

24 (*a*) A. Orte, J. M. Alvarez-Pez and M. J. Ruedas-Rama, *ACS Nano*, 2013, **7**, 6387–6395; (*b*) Y. Ning, S. Cheng, J.-X. Wang, Y.-W. Liu, W. Feng, F. Li and J.-L. Zhang, *Chem. Sci.*, 2019, **10**, 4227–4235; (*c*) J. J. Rennick, C. J. Nowell, C. W. Pouton and A. P. R. Johnston, *Nat. Commun.*, 2022, **13**, 6023.

25 (*a*) J. B. Grimm, L. M. Heckman and L. D. Lavis, *Prog. Mol. Biol. Transl. Sci.*, 2013, **113**, 1–34; (*b*) A. Nadler and C. Schultz, *Angew. Chem., Int. Ed.*, 2013, **52**, 2408–2410; (*c*) A. S. Klymchenko, *Acc. Chem. Res.*, 2017, **50**, 366–375; (*d*) D. Si, Q. Li, Y. Bao, J. Zhang and L. Wang, *Angew. Chem., Int. Ed.*, 2023, **62**, e20230764.

26 Probes for Lysosomes, Peroxisomes and Yeast Vacuoles—Section 12.3, in *The Molecular Probes Handbook*, ed. M. T. Z. Spence and I. D. Johnson, Thermo Fisher Scientific, 11th edn, 2010.

27 (*a*) S. S. Chauhan, X.-J. Liang, A. W. Su, A. Pai-Panandiker, D.-W. Shen, J. A. Hanover and M. M. Gottesman, *Br. J. Cancer*, 2003, **88**, 1327–1334; (*b*) N. Raben, L. Shea, V. Hill and P. Plotz, *Methods Enzymol.*, 2009, **453**, 417–449; (*c*) P. M. Haggie and A. S. Verkman, *J. Biol. Chem.*, 2009, **284**, 7681–7686; (*d*) D. M. Wolfe, J.-H. Lee, A. Kumar, S. Lee, S. J. Orenstein and R. A. Nixon, *Eur. J. Neurosci.*, 2013, **37**, 1949–1961; (*e*) J. Zeng, O. S. Shirihai and M. W. Grinstaff, *J. Life Sci.*, 2020, **2**, 25–37.

28 (*a*) S. Chow and D. Hedley, *Curr. Protoc. Cytom.*, 2001, **9**, PMID: 18770756; (*b*) L. Ma, Q. Ouyang, G. C. Werthmann, H. M. Thompson and E. M. Morrow, *Front. Cell Dev. Biol.*, 2017, **5**, 71.

29 A. Daina, O. Michielin and V. Zoete, *Sci. Rep.*, 2017, **7**, 42717.

30 (*a*) G. K. Vegesna, J. Janjanam, J. Bi, F.-T. Luo, J. Zhang, C. Olds, A. Tiwari and H. Liu, *J. Mater. Chem. B*, 2014, **2**, 4500–4508; (*b*) A. Mukherjee, P. C. Saha, R. S. Das, T. Bera and S. Guha, *ACS Sens.*, 2021, **6**, 2141–2146; (*c*) A. Mukherjee, P. C. Saha, S. Kar, P. Guha, R. S. Das, T. Bera and S. Guha, *ChemBioChem*, 2023, **24**, e20220064; (*d*) Z. Li, S. Yang, H. Xiao, Q. Kang, N. Li, G.-L. Wu, S. Tan, W. Wang, Q. Fu, X. Tang, J. Zhou, Y. Huang, G. Chen, X. Tan and Q. Yang, *Bioconjugate Chem.*, 2024, **35**, 1015–1023.

31 (*a*) O. G. Peterson, S. A. Tuccio and B. B. Snavely, *Appl. Phys. Lett.*, 1970, **17**, 245–247; (*b*) B. Wellegehausen, L. Laepple and H. Welling, *Appl. Phys.*, 1975, **6**, 335; (*c*) H. El-Kashef, *Physica B*, 2000, **279**, 295; (*d*) S. Sinha, A. Ray and K. Dasgupta, *J. Appl. Phys.*, 2000, **87**, 3222; (*e*) H. El-Kashef, *Physica B*, 2002, **311**, 376; (*f*) S. Sinha, A. K. Ray, S. Kundu, S. Sasikumar and K. Dasgupta, *Appl. Phys. B*, 2002, **75**, 85; (*g*) A. Sen, A. K. Mora, S. K. Agarwalla, G. Sridhar, S. Kundu and S. Nath, *Spectrochim. Acta, Part A*, 2022, **282**, 121642.

32 Laser & Fluorescent Dyes, Luxottica/Exciton, https://exciton.luxottica.com/laser-dyes.html, accessed 2024-10-26.

33 E. Avellanal-Zaballa, L. Gartzia-Rivero, T. Arbeloa and J. Bañuelos, *Int. Rev. Phys. Chem.*, 2022, **41**, 177–203.